Cell

A Signaling Principle for the Specification of the Germ Cell Lineage in Mice

Yasuhide Ohinata,[1] Hiroshi Ohta,[2] Mayo Shigeta,[1] Kaori Yamanaka,[1] Teruhiko Wakayama,[2] and Mitinori Saitou[1,3,4,*]
[1]Laboratory for Mammalian Germ Cell Biology
[2]Laboratory for Genomic Reprogramming
Center for Developmental Biology, RIKEN Kobe Institute, 2-2-3 Minatojima-Minamimachi, Chuo-ku, Kobe 650-0047, Japan
[3]Laboratory of Molecular Cell Biology and Development, Graduate School of Biostudies, Kyoto University, Yoshida-Konoe-cho, Sakyo-ku, Kyoto 606-8501, Japan
[4]Present address: Department of Anatomy and Cell Biology, Graduate School of Medicine, Kyoto University, Yoshida-Konoe-cho, Sakyo-ku, Kyoto 606-8501, Japan
*Correspondence: saitou@cdb.riken.jp
DOI 10.1016/j.cell.2009.03.014

SUMMARY

Specification of the germ cell lineage is vital to development and heredity. In mice, the germ cell fate is induced in pluripotent epiblast cells by signaling molecules, yet the underlying mechanism remains unknown. Here we demonstrate that germ cell fate in the epiblast is a direct consequence of Bmp4 signaling from the extraembryonic ectoderm (ExE), which is antagonized by the anterior visceral endoderm (AVE). Strikingly, Bmp8b from the ExE restricts AVE development, thereby contributing to Bmp4 signaling. Furthermore, Wnt3 in the epiblast ensures its responsiveness to Bmp4. Serum-free, defined cultures revealed that, in response to Bmp4, competent epiblast cells uniformly expressed key transcriptional regulators Blimp1 and Prdm14 and acquired germ-cell properties, including genome-wide epigenetic reprogramming, in an orderly fashion. Notably, the induced cells contributed to both spermatogenesis and fertility of offspring. By identifying a signaling principle in germ cell specification, our study establishes a robust strategy for reconstituting the mammalian germ cell lineage in vitro.

INTRODUCTION

The germ cell lineage is the source of totipotency, ensuring the creation of new organisms in most multicellular species. In mice, primordial germ cells (PGCs), which are the origin of both oocytes and spermatozoa, emerge from the proximal epiblast cells and arise as a cluster of approximately 40 alkaline-phosphatase (AP)-positive cells in the extraembryonic mesoderm at around embryonic day (E) 7.25 (Ginsburg et al., 1990; Lawson and Hage, 1994). Thereafter, they initiate migration, passing through a developing hindgut and colonizing the embryonic gonads, where they initiate differentiation into either oocytes or spermatozoa.

Gene-knockout studies have demonstrated that bone morphogenetic protein (Bmp) signals play essential roles in the generation of AP-positive PGCs from the epiblast (see review, (Saitou, 2009)): Bmp4 and Bmp8b emitted from the ExE, as well as the signal transducers known as Smads (Smad1, 4, and 5), are critical for the generation of PGCs. In addition, Bmp2 arisen from the VE seems to augment the role of Bmp4 to ensure the generation of sufficient numbers of PGCs. A Bmp ligand initiates signaling by binding to and bringing together type I (activin receptor-like kinase (Alk) 3/BmprIA, Alk6/BmprIB, and Alk2) and type II (Bmp type II receptor (BmprII) and activin type II receptors (ActrIIA and ActrIIB)) receptor serine/threonine kinases on the cell surface. This allows receptor II to phosphorylate the receptor I kinase domain, which then propagates the signal through phosphorylation of the conserved C-terminal residues of the Smad1, 5, or 8 proteins, which, by forming heterodimers with Smad4, translocate to the nucleus and function as transcriptional regulators (Shi and Massague, 2003). At present, however, the mechanism through which the Bmp signals generate the germ cell lineage (i.e., direct target cells, receptor complexes, and target genes employed by Bmps, etc.) and why only a subset of epiblast cells is specifically induced into germ cell fate remain largely unclear. Indeed, there exists a formal possibility that some unidentified secondary factor specifies the germ cell fate in the Bmp-sensitized epiblast cells (Lawson et al., 1999). Furthermore, other signaling pathways that play key roles during gastrulation, such as Wnt and Nodal signaling (Brennan et al., 2001; Liu et al., 1999), may be involved in germ cell specification.

Recent studies have identified B-lymphocyte induced maturation protein 1 (Blimp1, also known as Prdm1) and Prdm14, two of the PR (PRDI-BF1 and RIZ) domain-containing transcriptional regulators, as key factors for the specification of germ cell fate (Ohinata et al., 2005; Vincent et al., 2005; Yamaji et al., 2008). The expression of *Blimp1* and *Prdm14* starts independently in a few cells of the proximal posterior epiblast at around the pre/no to early-streak (P/0S-ES) stage (~E6.25-E6.5, see (Downs and Davies, 1993) for embryonic staging), and these cells increase in number and go on to form PGCs with AP activity and stella/*Pgc7* expression (Saitou et al., 2002; Sato et al.,

2002) at around the late-streak to early-bud (LS-EB) stage (E7.25). *Blimp1*-, *Prdm14*-, and stella-positive PGCs integrate three key events, the repression of a somatic mesodermal program (Saitou et al., 2002), re-acquisition of a potential pluripotency (Yabuta et al., 2006), and ensuing genome-wide epigenetic reprogramming during their migration period (Seki et al., 2007). Blimp1 is essential for all three events (Kurimoto et al., 2008), whereas Prdm14 ensures the latter two (Yamaji et al., 2008).

These advances in our understanding of the molecular properties of the emerging germ cell lineage have now made it possible to tackle some of the most important, yet unresolved questions: How do the signaling molecules in gastrulation endow a restricted population of the epiblast cells with the germ cell fate, and how would it be possible to induce the epiblast cells selectively toward the germ cell fate? In this study, through extensive in vivo genetic analyses as well as in vitro serum-free cultures, we have identified a paradigm of signaling activity for the specification of germ cell fate, highlighting the feasibility of generating the germ cell lineage in mammalian species in vitro.

RESULTS

Extraembryonic Signals Dictate the Induction of Germ Cell Fate

In contrast to the expression of *Blimp1* and *Prdm14*, which is restricted to the most proximal posterior epiblast cells at the P/0S-ES stage (Figures 1A and 1B, and Figure S1 available with this article online) (Ohinata et al., 2005; Yamaji et al., 2008), *Bmp4* and *Bmp8b*, key signals for the germ cell fate, are expressed uniformly in the ExE (Figure 1C; Lawson et al., 1999; Ying et al., 2000), leading us to speculate that germ cell induction in the epiblast may be regulated by two signaling axes, one reflecting a proximity to the ExE, the source of the Bmp signaling, and the other reflecting the posterior properties (Figure 1D).

To explore this possibility, we examined the expression of the *Blimp1* reporter, *Blimp1*-mVenus (BV) (Ohinata et al., 2008), in the mutants for *Bmp4*, *Bmp8b*, and *Smad1*. In all three homozygous$^{-/-}$ mutants, BV in the epiblasts was absent or severely impaired (Figures 1E–1H and S2), indicating that germ cell specification is blocked at its earliest stage in these mutants. All three $^{-/-}$ embryos failed to express *Prdm14*, as visualized by the *Prdm14*-mVenus (P14V) reporter (Figures 1I and S3; Yamaji et al., 2008). In both the *Bmp4*$^{-/-}$ and *Bmp8b*$^{-/-}$ mutants, epiblast cells lost the signal for the C-terminally phosphorylated, active form of Smad1/5/8 (pSmad1/5/8), which presented strongly both in the BV-positive cells and embryonic mesoderm in wild-type embryos (Figure 1E). In contrast, *Smad1*$^{-/-}$ epiblast cells showed some levels of the pSmad1/5/8 (Figure 1E), which would reflect the phosphorylated Smad5 (Arnold et al., 2006). These findings indicate that ExE-derived Bmp signals, through the phosphorylation of Smad proteins, directly or indirectly activate *Blimp1* and *Prdm14* in the most proximal epiblast cells.

We next analyzed *Blimp1* expression in the mutants for *Smad2* and *FoxH1* (Brennan et al., 2001; Nomura and Li, 1998; Yamamoto et al., 2001). Smad2 and FoxH1 mediate Nodal signaling, especially in the VE, and are required to form AVE, which emits inhibitory signals [e.g., Cer1 against Bmp and Nodal, Lefty1 against Nodal, Dkk1 against Wnt, etc.] ((Lewis et al., 2008; Perea-Gomez et al., 2002), for review see (Tam and Loebel, 2007)) against posteriorization, contributing to the anterior-posterior polarity of the early embryo. Consequently, in *Smad2*$^{-/-}$ embryos, the entire epiblast adopts a posterior mesodermal fate and, similarly, a substantial proportion of *FoxH1*$^{-/-}$ mutants failed to specify anterior structures. In both mutants, ExE seems relatively unaffected.

Remarkably, in *Smad2*$^{-/-}$ embryos that lack *Cer1*-positive AVE (but bear the BV-positive VE itself) (Figures 1J, 1K, and S4; Brennan et al., 2001), all the epiblast cells contacting the ExE, as well as those locating more distally, showed strong BV (Figures 1K and S4, second row). In severely affected *Smad2*$^{-/-}$ mutants, essentially all the epiblast-derived cells showed BV (Figures 1K and S5, third row). The numbers of BV-positive cells in the mutants were much larger than those in the wild-types (Figure 1L). Notably, thicker VE cells were observed at the distal part of some $^{-/-}$ mutants (Figure 1K, arrowhead): These would be aberrant distal VE (DVE)-like cells that failed to migrate anteriorly to become AVE. Similarly, in *FoxH1*$^{-/-}$ embryos, the BV-positive region expanded into a larger area of the epiblast (Figure 1K) and the numbers of BV-positive cells increased substantially (Figure 1M). We observed an increased number of BV-positive cells both in the *Smad2* and *FoxH1* heterozygous$^{+/-}$ mutants, especially at the early- to midstreak (E-MS, E6.5-E6.75) stages (t test, $p < 0.05$). In some *FoxH1*$^{-/-}$ mutants that developed relatively normally through gastrulation, we detected a much larger cluster of AP-positive cells (Figure S6) and of *Blimp1*- and stella-positive cells (Figure 1N) than those in wild-type embryos, suggesting that the excessive BV-positive mutant epiblast cells can differentiate into PGC-like cells. These findings indicate that the restricted expression of *Blimp1* in the posterior region is due to an inhibition of its expression in the anterior region by the AVE, and in its absence, most, if not all, of the PS stage epiblast cells can adopt the germ cell fate if they receive Bmp signals.

An In Vitro Serum-Free Culture for Germ Cell Induction from the Epiblast

To precisely define the roles of signaling molecules and the pathways for germ cell induction, we established a system for the serum- and feeder-free in vitro culture of early embryos. When cultured in GMEM with 15% KSR (hereafter referred to as serum-free basal medium (SFM), see Experimental Procedures) for 36 hr in a floating condition, E6.0 whole embryos, which showed BV only in the VE, developed into E7.5 embryo-like structures bearing a cluster of BV- and AP-positive PGC-like cells (Figures 2A and S7), suggesting that this condition allows normal embryonic development and germ cell specification.

Using this system, we examined the requirements of ExE and VE for *Blimp1* induction in the epiblast. E6.0 embryonic fragments bearing ExE and epiblasts (ExE+Epi, VE removed) showed BV relatively uniformly in the epiblast after 36 hr culture in the SFM (Figure 2A). When cultured with LIF, the epiblast cells still exhibited BV (Figure 2A). Notably, when cultured with LIF and BMP4, nearly all the epiblast cells showed strong BV (Figure 2A). These findings indicate that ExE induces *Blimp1* in the epiblast

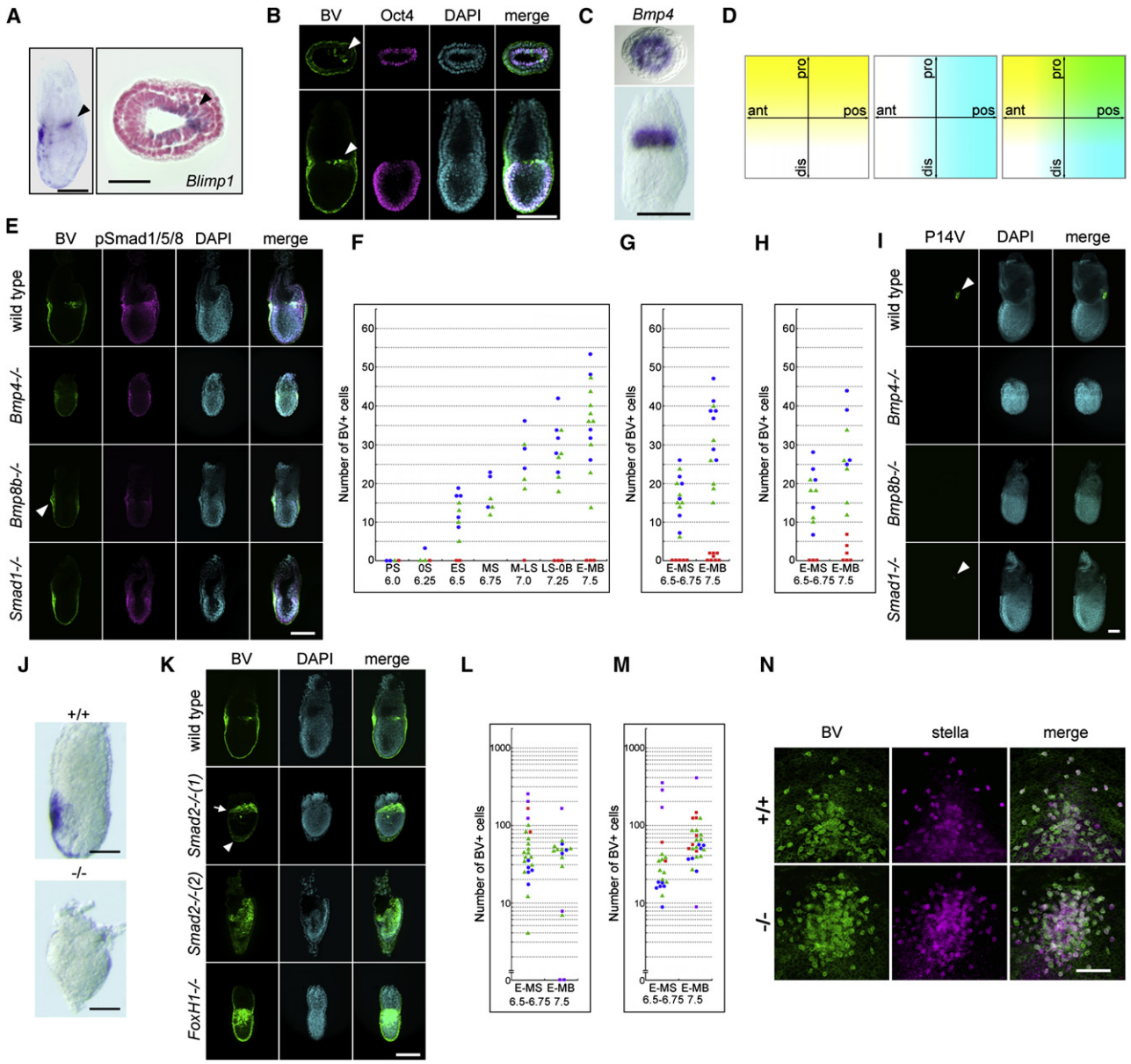

Figure 1. Influence of Extraembryonic Signals on Germ Cell Induction

(A and B) *Blimp1* expression in ES stage embryos. Arrowheads, *Blimp1*-positive epiblast cells. (A) In situ hybridization. Left, a lateral view. Anterior to the left. Bar, 100 μm. Right, a transverse section. The scale bar represents 50 μm. (B) BV counter-stained by Oct4 (magenta) and DAPI (cyan). Right, merge (also in E, I, K, and N). Top, transverse views. Bottom, sagittal views. Bars, 100 μm (also in subsequent panels).

(C) *Bmp4* in a P/0S stage embryo. Top, a transverse section. Bottom, a lateral view.

(D) Two signaling axes for PGC specification in the epiblast. Yellow, influence of signals from ExE. Blue, posterior properties. PGCs emerge where the two axes merge. Abbreviations are as follows: ant, anterior; pos, posterior; pro, proximal; dis, distal.

(E) BV and pSmad1/5/8 (magenta) in wild-type, *Bmp4*$^{-/-}$, *Bmp8b*$^{-/-}$, and *Smad1*$^{-/-}$ ES stage embryos, counter-stained with DAPI. The arrowhead indicates an abnormally thick AVE in the *Bmp8b*$^{-/-}$ embryos.

(F–H) Numbers of BV-positive cells in embryos from the PS to E-MB stages of *Bmp4* (F), *Bmp8b* (G), and *Smad1* (H) mutants. Blue circles, green triangles, and red squares represent the numbers of BV-positive cells in $^{+/+}$, $^{+/-}$, and $^{-/-}$ embryos, respectively, of each mutant.

(I) P14V (arrowheads) in wild-type, *Bmp4*$^{-/-}$, *Bmp8b*$^{-/-}$, and *Smad1*$^{-/-}$ EB stage embryos, counter-stained with DAPI.

(J) *Cer1* expression in *Smad2*$^{+/+}$ and $^{-/-}$ (severe) E-MS stage embryos.

(K) BV in wild-type, *Smad2*$^{-/-}$ (*1*, less severe), *Smad2*$^{-/-}$ (*2*, severe), and *FoxH1*$^{-/-}$ E-MS stage embryos, counter-stained with DAPI.

(L and M) Numbers of BV-positive cells in embryos at the E-MS and E-MB stages of *Smad2* (L) and *FoxH1* (M) mutants. Blue circles, green triangles, red squares, and purple squares represent the numbers of BV-positive cells in $^{+/+}$, $^{+/-}$, $^{-/-}$, and severely affected (type-II) $^{-/-}$ embryos, respectively, of each mutant. *Smad2* and *FoxH1*$^{+/-}$ mutants at the E/MS stages bear larger numbers of BV-positive cells than $^{+/+}$ littermates (t test, $p < 0.05$).

(N) Three-dimensionally reconstructed posterior views of BV- and stella- (magenta) positive cells in wild-type and *FoxH1*$^{-/-}$ embryos at E7.75.

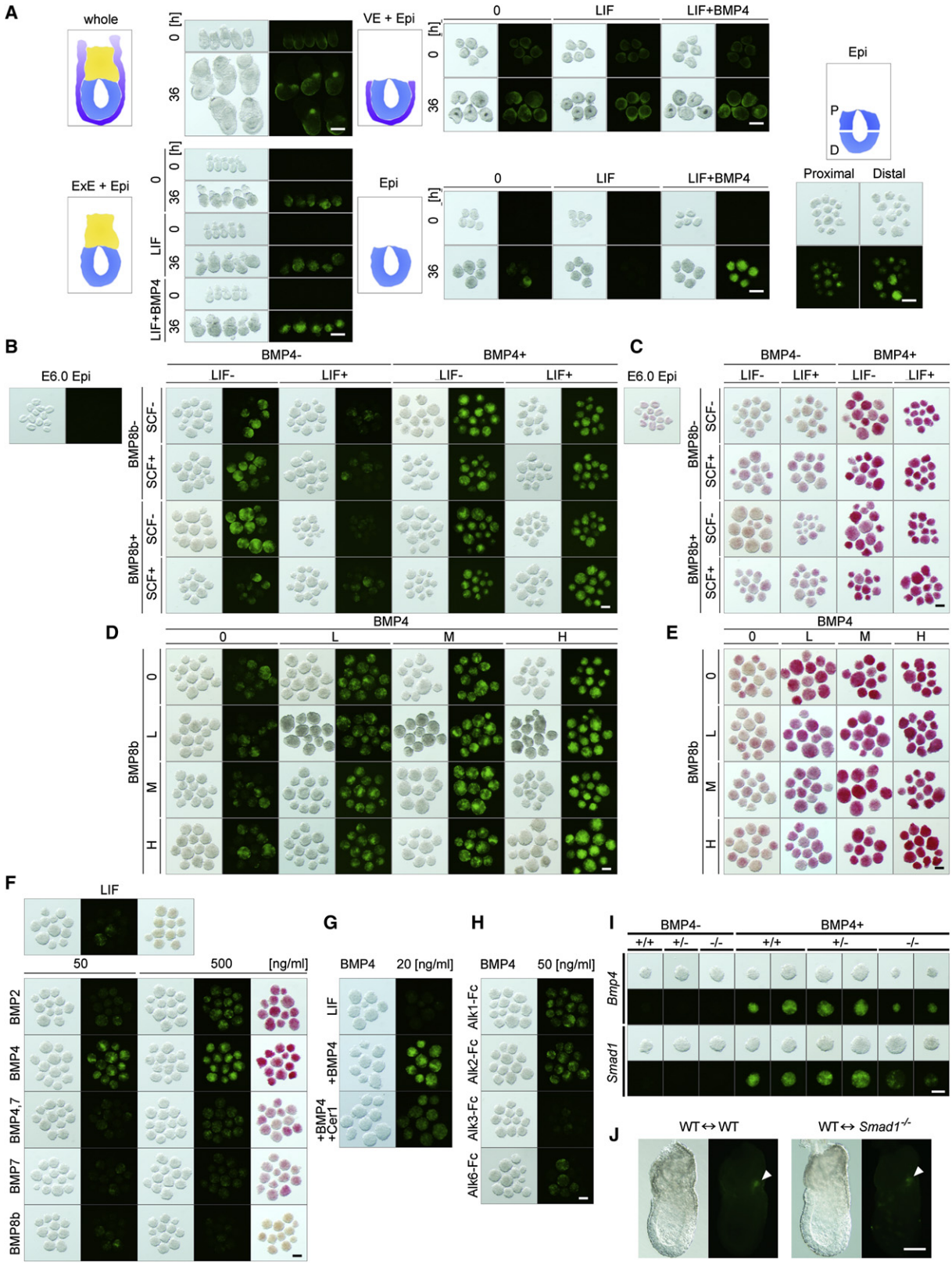
A
whole
ExE + Epi
VE + Epi
Epi
0 [h]
36
0
LIF
LIF+BMP4
Epi
P
D
Proximal
Distal
B
E6.0 Epi
BMP4-
BMP4+
LIF-
LIF+
BMP8b-
BMP8b+
SCF-
SCF+
C
D
BMP4
0
L
M
H
BMP8b
E
F
LIF
50
500
[ng/ml]
BMP2
BMP4
BMP4,7
BMP7
BMP8b
G
20 [ng/ml]
+BMP4
+BMP4 +Cer1
H
50 [ng/ml]
Alk1-Fc
Alk2-Fc
Alk3-Fc
Alk6-Fc
I
+/+
+/-
-/-
Bmp4
Smad1
J
WT ↔ WT
WT ↔ Smad1-/-

without VE and that exogenous BMP4 further potentiates *Blimp1* induction. In contrast, E6.0 embryonic fragments bearing VE and Epi (ExE removed) did not exhibit BV in the epiblast under any of the three conditions (Figure 2A). This may be because ExE may secrete some factor(s) other than BMP4, which is (are) indispensable for *Blimp1* expression in the epiblast, or VE, more specifically AVE, may function as an inhibitor of *Blimp1* induction in this condition, as indicated by the genetic experiments. To distinguish between these possibilities, we cultured isolated epiblasts (Epi, VE and ExE removed). After 36 hr culture in the SFM, the epiblasts appeared to show good growth and, unexpectedly, some BV (Figure 2A). However, when cultured with LIF, they grew similarly but did not show BV (Figure 2A). We found that LIF has an activity to suppress the induction of *Goosecoid* (*Gsc*), a marker for the mesendoderm (see review, Tam and Loebel, 2007; Figure S8), suggesting that *Blimp1* expression in the SFM might reflect a differentiation of epiblast cells into a mesendodermal lineage. We then cultured the epiblasts (the entire epiblast, as well as the proximal and distal halves) with LIF and BMP4 and found that all these fragments exhibited intense BV (Figure 2A). These data indicate that essentially all the epiblast cells at E6.0, if separated from VE, a source for inhibitory signals, are able to express *Blimp1* in response to BMP4 alone.

BMP4 Is Sufficient to Induce PGC-like Cells from the Epiblast

By using *Blimp1*, *Prdm14*, and AP activity as markers for PGCs, we next explored the conditions for PGC specification. In addition to LIF and BMP4, we examined the effects of BMP8b, SCF, a potent survival factor of PGCs (Dolci et al., 1991; Matsui et al., 1991), and other BMPs.

Epiblasts cultured in the SFM for 36 hr showed BV, but they were negative for AP activity, and thus were not PGC-like cells (Figures 2B and 2C). No induction of BV- or AP-positive cells was observed in response to addition of SCF, BMP8b or both (Figures 2B and 2C). When LIF was added, BV was suppressed, but again, addition of SCF, BMP8b or both did not induce BV- and AP-positive cells (Figure 2B, C). In contrast, epiblasts cultured in the SFM with BMP4 exhibited BV and AP activity with high efficiency, regardless of the presence of LIF, SCF, or BMP8b (Figures 2B and 2C). These findings indicate that BMP4 alone can induce essentially all the E6.0 epiblast cells into *Blimp1*- and AP-positive PGC-like cells. Addition of LIF would theoretically be beneficial for PGC-like cell culture, since LIF promotes PGC growth (Dolci et al., 1991; Matsui et al., 1991), and inhibits the entry of PGCs into meiosis (Farini et al., 2005) (see also above). It was essential to culture the epiblasts in a serum-free, floating condition to induce PGC-like cells, since addition of 5% FBS or adherent culture in a fibronectin-coated dish prevented BV induction (Figure S9).

We next examined the dose-dependent effect of BMP4 by culturing E6.0 epiblast with varying concentrations of BMP4 and BMP8b: The efficiency of BV and AP activity induction was highly dependent on the dosage of BMP4, but not of BMP8b (Figures 2D and 2E). We evaluated the effects of a panel of BMPs and found that BMP4 and BMP2 were the most and second-most potent inducers, respectively, of the BV- and AP-positive PGC-like cells (Figure 2F). Importantly, we obtained identical results on the induction of *Prdm14* in isolated epiblasts (Figures S10 and S11). Furthermore, consistent with the idea that AVE inhibits *Blimp1* expression, exogenous Cer1, one of the inhibitory signals from the AVE, blocked BMP4-mediated BV induction from the epiblast (Figure 2G). These findings demonstrate that BMP4 but not BMP8b is sufficient to induce *Blimp1*-, *Prdm14*-, and AP-positive PGC-like cells from the epiblast dose-dependently in culture.

A Signaling Pathway for *Blimp1* and *Prdm14* Induction by Bmp4

We next analyzed a signaling pathway for *Blimp1* and *Prdm14* induction by Bmp4. We evaluated the effect of Alks-Fc fragments on BV and P14V induction by BMP4, revealing that the Alk3- and Alk6-Fc fragments are the most and second-most potent inhibitors, respectively (Figures 2H and S11). We tested whether the *Bmp4*$^{-/-}$ and *Smad1*$^{-/-}$ epiblasts can respond to BMP4. Remarkably, *Bmp4*$^{-/-}$ epiblasts exhibited BV and P14V in response to BMP4 (Figures 2I and S12), indicating that the lack of BV and P14V in the *Bmp4*$^{-/-}$ epiblasts is due solely to the loss of Bmp4 in the ExE. In contrast, *Smad1*$^{-/-}$ epiblasts were resistant to BMP4 for BV and P14V expression, although weak and sporadic inductions of these genes were detected, presumably due to the presence of Smad5 (Figures 2I and S12).

A previous work has reported that Bmp4 signaling through Alk2 and Smad1 in the VE is an obligatory pathway for the generation of AP-positive PGCs (de Sousa Lopes et al., 2004). However, our evidence indicates that Bmp4 signaling through Alk3 (or Alk6) via Smad1 (and 5) in the epiblast is sufficient to induce *Blimp1*-, *Prdm14*-, and AP-positive PGC-like cells in vitro and that the (A)VE works, at least in part, as a source for inhibitory signal(s) against Bmp4 for *Blimp1* induction. We

Figure 2. A Serum-free Culture for Germ Cell Induction from the Epiblast

(A) 36 hr cultures of BV-bearing whole (top, left), VE (dark blue)-removed (bottom, left), ExE (yellow)-removed (top, middle), VE- and ExE-removed (Epi only, blue) (bottom, middle) embryos in the SFM with LIF (1000 U/ml) or LIF+BMP4 (500 ng/ml). Right, 36 hr cultures of BV-bearing proximal (P) or distal (D) epiblasts with LIF and BMP4. 0, at the onset of cultures; 36, after 36 hr cultures. Bright-field and Venus fluorescence are shown (also in B, D, F-J). Bars, 100 μm (also in subsequent panels).

(B and C) Effects of BMP4 (500 ng/ml), BMP8b (500 ng/ml), LIF (1000 U/ml), and SCF (100 ng/ml) on BV (B) and AP-activity (C) induction after 36 hr culture. +, presence of the indicated factors; −, absence of the indicated factors.

(D and E) Dose-dependent effects of BMP4 and BMP8b on BV (D) and AP-activity (E) induction after 36 hr cultures in the SFM with LIF and SCF. 0, no cytokines; L, 20 ng/ml; M, 100 ng/ml; H, 500 ng/ml.

(F–H) Effects of a panel of BMPs (indicated concentrations) on BV and AP-activity induction (F), effects of Cer1 (1 μg/ml) (G) and of Alks-Fc fragments (1 μg/ml) (H) on BV induction by BMP4 after 36 hr culture in the SFM with LIF.

(I) Effects of BMP4 (BMP4+, 500 ng/ml) on BV induction in *Bmp4* or *Smad1*$^{+/+}$, $^{+/-}$ and $^{-/-}$ embryos.

(J) Chimeras between wild-type (WT, left) or *Smad1*$^{-/-}$ (right) blastocysts and wild-type ES cells with BV developed to the 0B stage. Arrowheads, BV-positive cells.

therefore examined whether Bmp4 signaling through Smad1 in the VE is obligatory for *Blimp1* expression in the epiblast by generating chimeras between blastocysts from *Smad1*$^{+/-}$ crosses and wild-type ES cells bearing the BV transgene: ES cells injected into blastocysts contribute only to the embryonic lineages (Nagy et al., 2003), and thus if the host blastocyst is *Smad1*$^{-/-}$, we can analyze whether Smad1 in the ExE and VE is obligatory for *Blimp1* expression in the epiblast. All chimeras between wild-type (n = 5), *Smad1*$^{+/-}$ (n = 8), and *Smad1*$^{-/-}$ (n = 2) hosts and ES cells with BV exhibited specific BV expression in the presumptive PGC precursors, but not in the VE (Figure 2J), demonstrating that Smad1 in the VE is dispensable for *Blimp1* expression in the epiblast. Thus, direct Bmp4 signaling in the epiblast through Alk3 (or Alk6) and one of the type II receptors complex via Smad1 and 5 is necessary and sufficient for PGC specification.

Time Window for Adoption of the Germ Cell Fate by Epiblast Cells

We next analyzed the time window for adoption of the germ cell fate by epiblast cells. Epiblasts isolated as early as E5.5 exhibited robust BV and AP activity in response to BMP4, whereas those isolated 6 hr earlier (E5.25) did not (Figure 3A). Until about E6.25, isolated epiblasts showed BV and AP activity, but those isolated at E6.5 or later exhibited less intense BV and weak/faint AP activity (Figure 3A). Thus, the epiblasts acquire the ability to adopt a *Blimp1*- and AP-positive PGC-like state in response to BMP4 at around E5.5 and lose it after around E6.5.

How long, then, is the period of time during which the *Blimp1*-positive cells are newly recruited from the epiblast for the germ cell fate in vivo? To address this question, we made use of a cell tracking method by a photo-convertible fluorescent reporter, KikGR (Tsutsui et al., 2005). KikGR is fluorescent green after synthesis but, by blue-violet light, can be converted to red, which persists permanently, serving as a lineage tracer. We generated a transgenic strain expressing membrane-targeted KikGR (mKikGR) under the control of *Blimp1* (BKik, Figure S13) and analyzed the recruitment of *Blimp1*-positive cells from the epiblast during critical periods for germ cell specification (Figures 3B and 3C). BKik embryos at the PS stage showed green fluorescence only in the VE, which was converted to red by violet light. The embryos were then cultured for 12 hr, reaching the 0S stage. As expected, the VE cells showed both green and red fluorescence, reflecting the newly synthesized and originally presented proteins, respectively (Figure 3C). Importantly, in the most proximal epiblasts, we observed a number of green-only cells, which represent newly recruited *Blimp1*-positive PGC precursors (Figure 3C). We performed the same experiment with the MS stage embryos, which, after culture, developed into EB stage embryos bearing cells with both green and red fluorescence ("labeled" cells at the MS stage) and with green-only fluorescence (newly recruited cells during the culture) (Figure 3C). We obtained a similar result with the LS stage embryos (Figure 3C). However, the EB stage embryos, which, after culture, developed into those of the late-head-fold (LHF) stage, bore cells only with both green and red fluorescence (Figure 3C). These findings show that the recruitment of the *Blimp1*-positive PGC precursors begins between the PS and 0S stages and continues at least until the LS stage, but after the EB stage, it apparently ceases and PGCs increase their numbers solely by cell division.

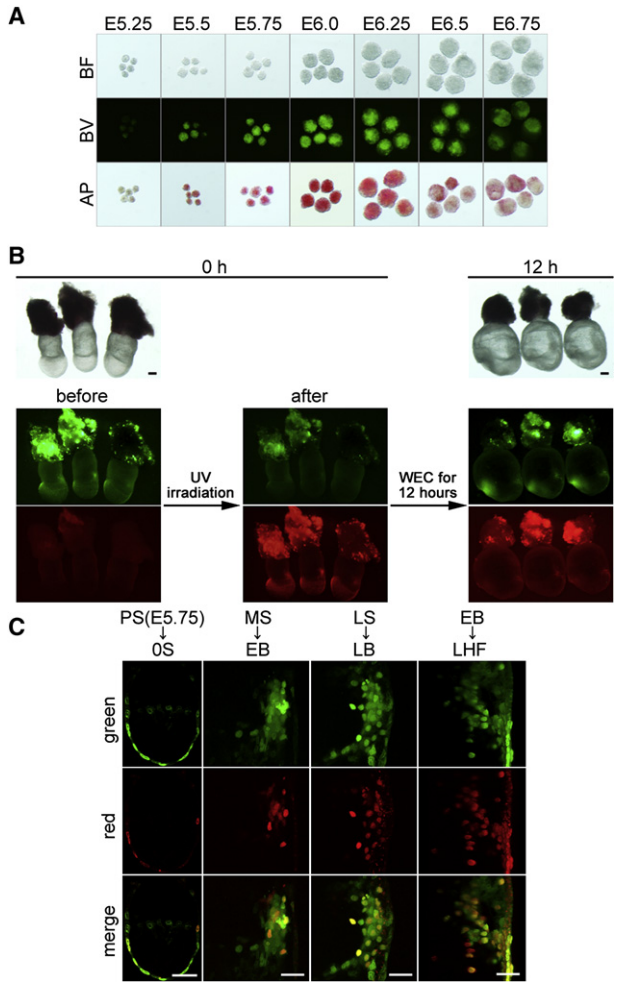

Figure 3. Competence of the Epiblast for a Germ Cell Fate

(A) Effects of BMP4 on BV and AP activity induction at differing developmental stages after 36 hr culture in the SFM with LIF. Top, bright-field images.

(B) EB stage BKik embryos, which showed green fluorescence (before, left) but were photo-converted to exhibit red fluorescence by blue-violet light (λ = 405 nm) irradiation (after, middle), were cultured for 12 hr, developed into the LHF stage (right), and showed green fluorescence by newly synthesized Kik and red fluorescence by the old Kik. Bar, 100 μm.

(C) BKik embryos at differing stages, photo-converted to show red fluorescence, were cultured for 12 hr, reaching the indicated stages. Newly-synthesized green and old red fluorescence as well as the merge are shown. The scale bars represent 50 μm.

Bmp8b Restricts AVE Development

What, then, would be the role of Bmp8b in PGC specification? We explored two possibilities—that Bmp8b is critical 1) for the proper expression of *Bmp4* in the ExE, or 2) for conferring to the epiblasts an ability to respond to Bmp4. However, our experiments negated both these functions (Figures 4B, 4C, and S12).

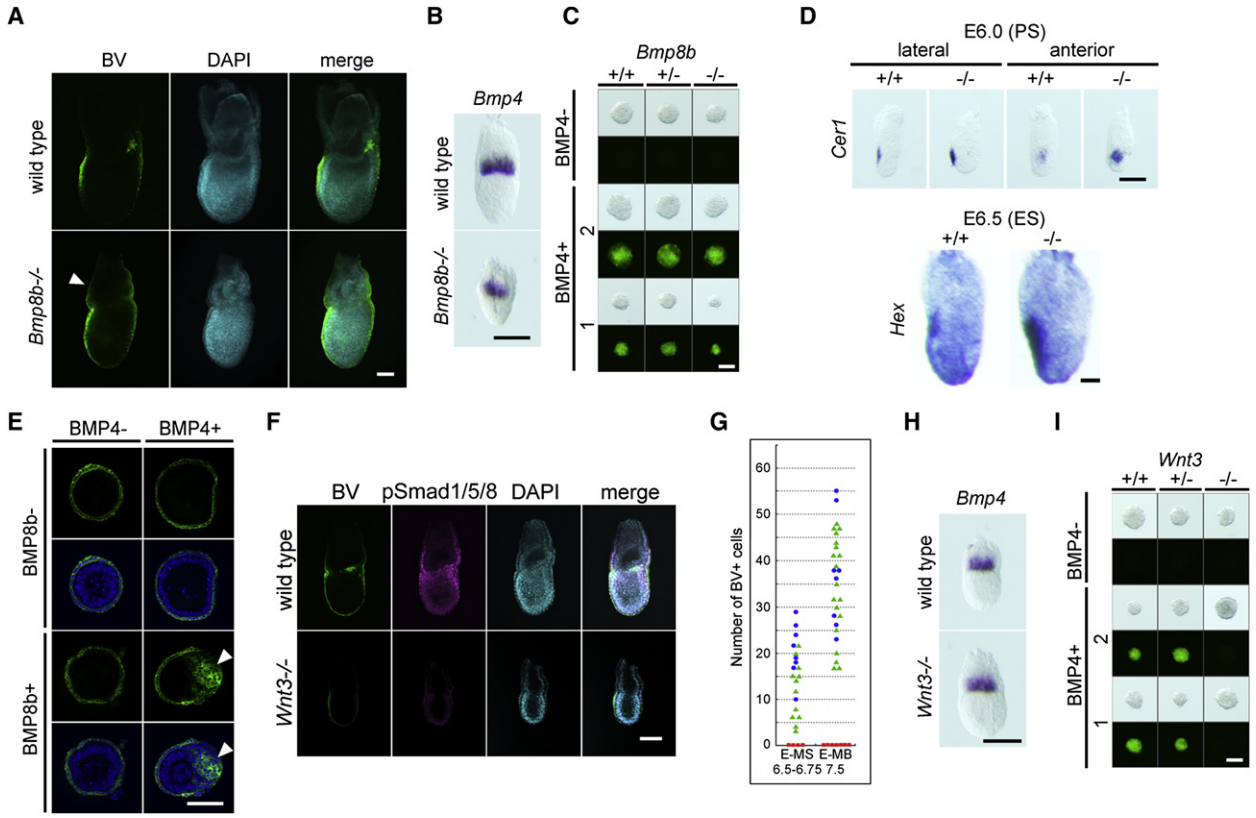

Figure 4. Roles of Bmp8b and Wnt3 on Germ Cell Induction

(A) BV in wild-type and *Bmp8b*$^{-/-}$ E-MB stage embryos, counter-stained with DAPI. Right, merge (also in [F]). The arrowhead indicates abnormal BV in the VE covering the ExE. Bar, 100 μm (also in subsequent panels).

(B) *Bmp4* in P/OS stage *Bmp8b*$^{+/+}$ and $^{-/-}$ embryos.

(C) Effects of BMP4 (BMP4+, 500 ng/ml) on BV induction in *Bmp8b*$^{+/+}$, $^{+/-}$ and $^{-/-}$ E6.0 epiblasts (two each, 1, 2). Bright-field (upper rows) and Venus fluorescence (lower) are shown (also in I).

(D) *Cer1* (PS stage, lateral and anterior views, top) and *Hex* (ES stage, bottom) in *Bmp8b*$^{+/+}$ and $^{-/-}$ embryos.

(E) Effects of BMP4 (500 ng/ml) and BMP8b (500 ng/ml) on BV induction from the E6.0 VE+Epi fragments after 36 hr culture in the SFM with LIF. Confocal images with BV and merges with DAPI (second and bottom rows) are shown. Arrowheads, BV in the epiblasts.

(F) BV and pSmad1/5/8 in E-MS stage wild-type and *Wnt3*$^{-/-}$ embryos, counter-stained with DAPI.

(G) Numbers of BV-positive cells in embryos at the E-MS and E-MB stages of *Wnt3* mutants. Blue circles, green triangles, and red squares represent the numbers of BV-positive cells in $^{+/+}$, $^{+/-}$, and $^{-/-}$ embryos, respectively.

(H) *Bmp4* expression in P/OS stage *Wnt3*$^{+/+}$ and $^{-/-}$ embryos.

(I) Effects of BMP4 (BMP4+, 500 ng/ml) on BV induction in E6.0 *Wnt3*$^{+/+}$, $^{+/-}$ and $^{-/-}$ epiblasts (two each, 1, 2).

We therefore examined a third possibility, that Bmp8b may control VE development, thereby modulating the inhibitory activity of the AVE against Bmp4. Indeed, we noted that *Bmp8b*$^{-/-}$ embryos exhibited unusual VE morphology, with BV expression extending abnormally to the extraembryonic parts (Figures 1E, S2, 4A, and S14). By analyzing the expression of *Cer1* and *Hex*, key AVE markers (Tam and Loebel, 2007; Thomas et al., 1998), we found that, compared to the wild-types, *Bmp8b*$^{-/-}$ embryos exhibited an expanded *Cer1* and *Hex* domain (Figure 4D).

We then evaluated the effect of Bmp8b on *Blimp1* induction in the Epi + VE culture. In this culture, even in the presence of BMP4, we did not detect BV in the epiblast (Figure 2A). In contrast, when we added BMP8b with BMP4, significant upregulations of pSmad1/5/8 and BV were detected in the epiblast (Figure 4E and data not shown). Collectively, these findings led us to conclude that Bmp8b from the ExE restricts the AVE development, confining the AVE-derived inhibitory signals against Bmp4 (and other factors such as Wnt and Nodal) to an appropriate level.

Wnt3 Provides Epiblast Cells with the Ability to Respond to Bmp Signals

We then explored the role of Wnt3, a key signal for early embryonic patterning (Liu et al., 1999), in germ cell specification: BV and P14V in the epiblasts and BV in the VE were absent or highly reduced, respectively, in the *Wnt3*$^{-/-}$ mutants (Figures 4F, 4G, and S15, and data not shown). Consistently, pSmad1/5/8 was nearly absent both in the epiblast and VE in these mutants, indicating the severe impairment of Bmp signaling in the absence of

Wnt3. *Wnt3*-deficient embryos expressed *Bmp4* in their ExE, but their epiblast cells at E6.0 were unable to express BV and P14V in response to BMP4 (Figures 4H, 4I, and S12). Since Wnt3a by itself did not induce BV in wild-type epiblasts (Figure S16), we conclude that Wnt3 is essential to provide epiblasts with the ability to respond to Bmp4 and thereby take on the germ cell fate. The potential involvement of Nodal in PGC specification is discussed in Figure S17 and its legend.

Robust Induction of PGC-like Cells from the Epiblast

We have so far provided evidence that isolated epiblasts can be induced to form *Blimp1*-, *Prdm14*-, and AP-positive PGC-like cells after 36 hr in a serum-free culture with BMP4. To explore whether these PGC-like cells truly bear properties equivalent, if not identical, to PGCs, we went on to analyze the effects of culture for longer periods. Cultured epiblasts with LIF, SCF, and BMP4 continued to express BV at a high ratio at least until 132 hr (132 hr from E6.0 corresponds to E11.5) (Figure 5A). To evaluate whether these PGC-like cells develop in a chronologically appropriate manner, we examined the expression of stella using stella-Venus (SV) and stella-ECFP (SC) reporters: SV and SC can be detected from E8.5 and E9.5, respectively, in PGCs (Ohinata et al., 2008). Notably, the cultured epiblasts began to show SV and SC at around after 60 hr and 84 hr, respectively, and maintained SV and SC at a high ratio at least until 132 hr (Figure 5A and data not shown), demonstrating a chronologically proper development of the PGC-like cells. We noted, however, that, under this condition, the growth of the PGC-like cells was somewhat poor: After 132 hr culture, epiblast-derived cells grew from ~250 to ~750 cells and approximately 400 cells (~55%) ended up with those with BV (Figures 5B–5D), a number much smaller than that of PGCs at the corresponding stage (~5,000 to ~10,000 at E11.5 (Tam and Snow, 1981)). We therefore examined the effects of additional cytokines and found that combinatorial addition of BMP8b and EGF (but not FGFs) with BMP4, LIF, and SCF had the most potent effect on the growth of the epiblast-derived cells; they grew from ~250 cells up to ~3000 cells and the total number of the BV-positive cells increased to ~1250 (~45%) (Figures 5B–5D, S18, and S19).

We then explored whether the *Blimp1*-positive cells that appeared under this condition exhibited proper PGC characteristics. We exploited the epiblasts bearing both the BV and SC transgenes to find that BV-expressing cells exclusively showed SC (Figure 5E). Similarly, epiblasts bearing both P14V and SC exhibited robust co-expression of P14V and SC (Figure 5E). The BVSC- or P14VSC-positive cells tended to localize on a part of the outer surface of the developing epiblasts, and this region was strongly positive for the AP activity (Figure 5E). Notably, 132 hr cultures of the BVSC epiblasts from different stages confirmed that the competence of the epiblasts for the germ cell fate was restricted between E5.5 and E6.25 (Figure 5F). BV-positive cells were specifically positive for Oct4, Sox2, AP activity, SSEA1, and mouse vasa homolog (Mvh) (Figure 5G). RT-PCR analysis of the entire culture showed that they additionally expressed *Nanog*, *Kit*, *nanos3*, and *Dnd1*, but were negative for *Sycp1*, a key marker for meiotic germ cells (Figure 5H). We then evaluated epigenetic properties of the PGC-like cells: They exhibited highly reduced genome-wide H3K9me2 and, instead, upregulated H3K27me3 (Figure 5I), which findings are in good agreement with those of PGCs after E9.5 (Seki et al., 2007). Furthermore, the PGC-like cells repressed Dnmt3b (Figure 5I), a key de novo DNA methyltransferase specifically downregulated in PGCs (Kurimoto et al., 2008).

Collectively, these data show that the competent epiblasts can be robustly induced, in a chronologically appropriate manner, into PGC-like cells (hereafter referred to as epiPGCs) bearing essential genetic and epigenetic properties representative of the premeiotic PGCs in a defined, serum-free culture (see below). The BVSC-positive state can be maintained up to 180 hr (Figure S20).

epiPGCs Can Form Functional Sperm In Vivo

PGCs are the precursors of gametes. Having established a culture system of directional epiPGC induction, we set out to examine if epiPGCs can form functional gametes in vivo, using two methodologies: Gonad reconstruction and seminiferous tubule injection (see Experimental Procedures) (Chuma et al., 2005).

First, we induced 43 E6.0 epiblasts bearing *acro/act*-EGFP (Ohta et al., 2000) to epiPGCs by culturing with BMP4, LIF, SCF, BMP8b, and EGF for 84 hr. The induced cells, which showed *Blimp1*, *Prdm14* expression and AP activity (Figure S21), were used to form four reconstructed gonads (~7,000 estimated PGC-like cells/gonad), which were then transplanted under the tunica albuginea of germ cell-depleted adult testes of the nude mice. We set up two negative controls: The E6.0 epiblasts without the epiPGC induction (46 epiblasts, ~2000 cells/gonad) and epiblasts cultured without BMP4 but with all the other factors for 84 hr (51 epiblast-derivatives, ~15000 cells/gonad; they were negative for *Blimp1*, *Prdm14*, and AP activity) (Figure S21). Ten weeks after transplantation, we isolated the reconstructed gonads to find that out of 4 gonads reconstructed using epiPGCs, 2 showed prominent donor-derived GFP-positive foci, which were representative of proper spermatogenesis (Figures 6A–6C and Table S1). In contrast, although some gonads with control cells showed some GFP-positive foci, these consisted of cells with a nongerm cell-like appearance (Figures 6A–6C and Table S1).

Second, we induced 122 epiblast cells to epiPGCs for 132 hr and then injected dissociated cells into 16 neonatal testes of W/W^v mice (~10,000 PGC-like cells/testis). As a positive and a negative control, we used male genital ridges at E12.5 (21 genital ridges, ~30,000 PGCs/testis) and E6.0 epiblasts without the induction (85 epiblasts, ~2,500 cells/testis), respectively. 3 testes out of 8 injected with cells from E12.5 genital ridges exhibited contribution of the donor cells to the spermatogenesis, whereas none of the testes injected with dissociated E6.0 epiblast cells did so, with one showing overt teratoma formation (Table S4 and Figure 6D). Among 16 testes injected with epiPGCs, one showed intense GFP-positive focus of proper spermatogenesis (Figures 6D, 6G, 6H, and Table S4).

We injected the spermatozoa and elongated spermatids derived from the GFP-positive epiPGCs in the reconstituted gonads or the W/W^v testis into the cytoplasm of oocytes at meiosis II (intracytoplasmic sperm injection, ICSI), which resulted in embryogenesis, forming 2-cell stage embryos with

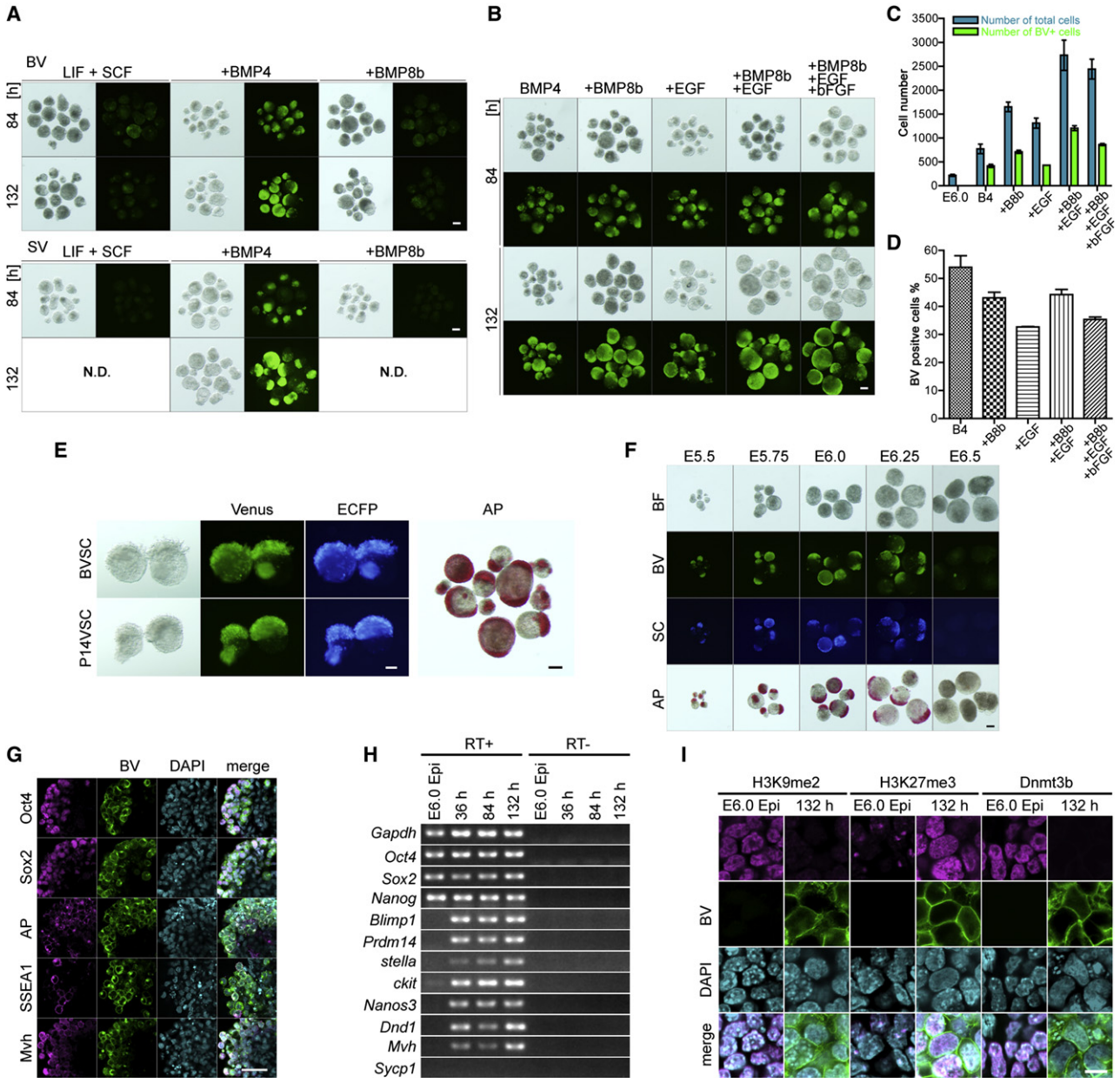

Figure 5. Robust Induction of PGC-like Cells from the Epiblast

(A) Effects of BMP4 (500 ng/ml), BMP8b (500 ng/ml), LIF (1000 U/ml), and SCF (100 ng/ml) on BV and SV induction in 84- and 132 hr cultures in the SFM. +BMP4 or +BMP8b, in addition to LIF and SCF. Bright-field and Venus fluorescence are shown (also in B). N.D., not determined. The scale bars represent 100 μm (also in subsequent panels except I).

(B–D) Effects of BMP4 (500 ng/ml), BMP8b (500 ng/ml), EGF (50 ng/ml), and basic FGF (bFGF) (50 ng/ml) on BV induction and growth of the epiblast-derived cells in 84- and 132 hr cultures. All the cultures include LIF (1000 U/ml) and SCF (100 ng/ml). (B) +, in addition to BMP4. (C) Numbers of total epiblast-derived cells (blue bars) and BV-positive cells (green) after 132 hr culture under the indicated conditions. Average numbers and standard deviations from three independent experiments (12 epiblasts/experiment) are shown. (D) Ratio of BV-positive cells to total epiblast cells in (C).

(E) BVSC, P14VSC, and AP activity of the epiblasts cultured in SFM with LIF (1000 U/ml), SCF (100 ng/ml), BMP4 (500 ng/ml), BMP8b (500 ng/ml), and EGF (50 ng/ml) for 132 hr.

(F) Induction of BV, SC and AP-activity from the epiblasts of differing developmental stages after 132 hr culture in the SFM with LIF (1000 U/ml), SCF (100 ng/ml), BMP4 (500 ng/ml), and BMP8b (500 ng/ml). Top, bright-field images.

(G–I) Gene expression and epigenetic properties of induced PGC-like cells as in (E). (G) BV-positive cells express Oct4, Sox2, AP-activity, SSEA1, and Mvh. Third column, DAPI, right, merge. (H) Gene expression of E6.0 epiblasts, and epiblasts cultured for 36, 84, and 132 hr as in (E) analyzed by RT-PCR. (I) BV-positive cells showed reduced H3K9me2, elevated H3K27me3, and repressed Dnmt3b, compared to E6.0 epiblasts. Third row, DAPI, bottom, merge. Bar, 100 μm.

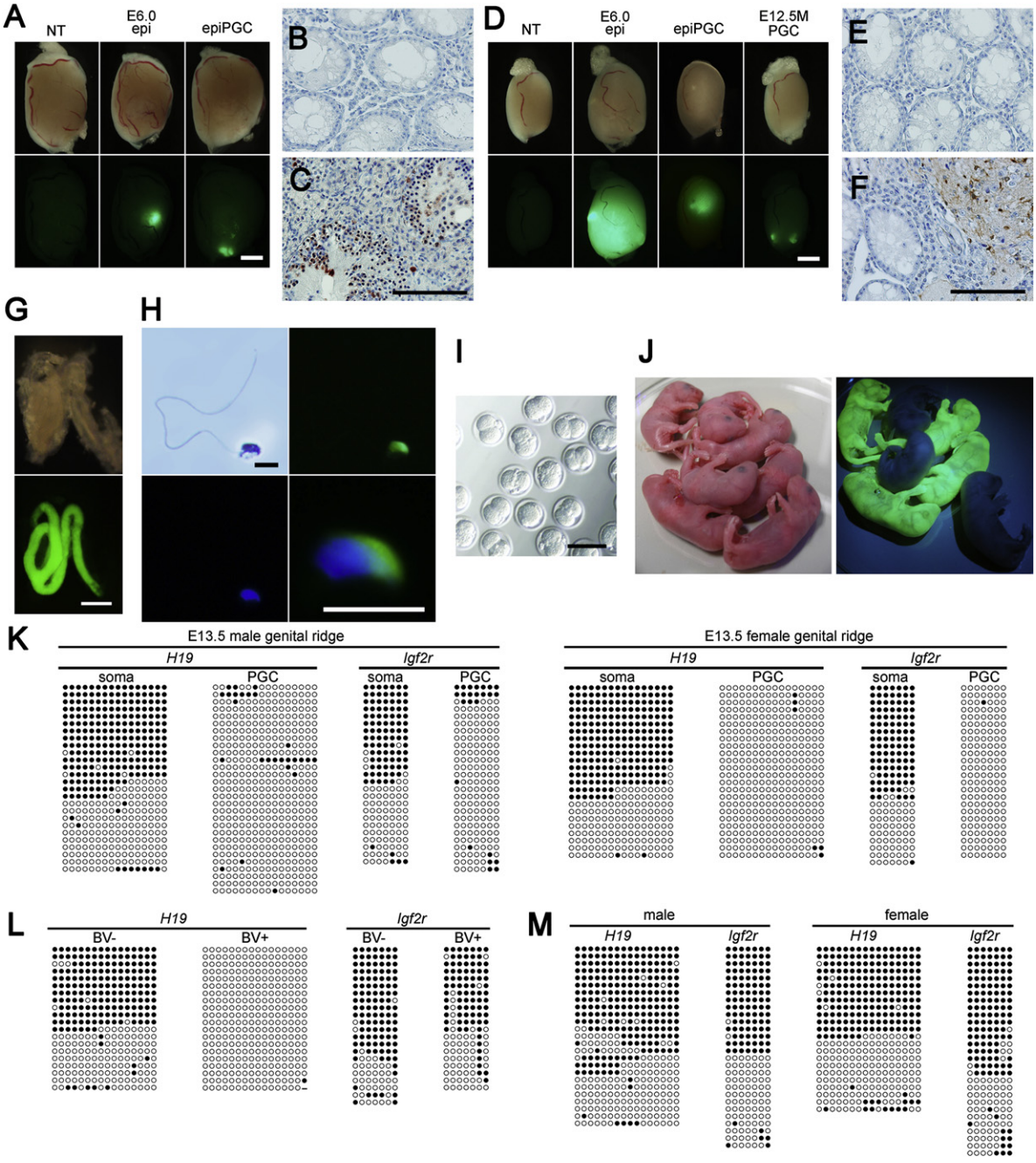

Figure 6. Functional Spermatogenesis by the epiPGCs

(A) Germ cell-depleted nude mice testes (no-transplantation (NT) control) grafted with reconstructed gonads with E6.0 epiblasts or induced epiblasts for 84 hr. Top row, bright-field; bottom, EGFP fluorescence (also in D and G). The scale bar represents 1 mm.

(B and C) Histology and immunostaining for EGFP (C) of the grafted testes shown in (A), counter-stained by hematoxylin. (B) The depleted, NT testis. (C) Spermatogenesis by the epiPGCs with EGFP immunoreactivity. The scale bar represents 100 μm.

(D) Neonatal testes of *W/W*^{v} mice (NT) directly transplanted with E6.0 epiblasts, epiblasts induced for 132 hr, and PGCs from E12.5 male gonads. Note the prominent EGFP signals in an epiblast-transplanted testis derived from teratoma. The scale bar represents 1 mm.

(E and F) Histology and immunostaining for EGFP (F) of the transplanted testes shown in (D), counter-stained by hematoxylin. (E) The NT testis. (F) A portion of teratoma by the donor epiblast cells with EGFP immunoreactivity. The scale bar represents 100 μm.

(G) A seminiferous tubule contributed by epiPGCs as in (D, third column). The scale bars represent 500 μm.

(H) A spermatozoon from an epiPGC. Top left, bright-field; bottom left, DAPI; top right, EGFP; bottom right, merge with higher magnification. EGFP is targeted to acrosome. The scale bars represent 10 μm.

(I) 2-cell embryos from the epiPGC-derived sperm. The scale bar represents 100 μm.

good efficiency (Figure 6I and Tables S2 and S5). We transferred these embryos to foster mothers and obtained healthy offspring, about half of which, as expected from the hemizygosity of the transgenes, showed green fluorescence (Figure 6J and Tables S3 and S6). These offspring grew apparently normally and became fully fertile (data not shown). Thus, the epiPGCs, but not the original epiblast cells or the cultured BV-negative cells, have the ability to generate proper gametes both in the reconstructed gonads and germ cell-deficient *W/W^{v}* testis.

Finally, we analyzed the imprinting methylation profiles of *H19* (paternally imprinted) and *Igf2r* (maternally imprinted) of epiPGCs induced for 132 hr and the offspring from these cells. Interestingly, sorted epiPGCs exhibited complete erasure of the imprints of *H19*, although they still maintained those of *Igf2r* (Figures 6K and 6L), whereas the BV-negative cells retained the imprints of both *H19* and *Igf2r* (Figure 6L). On the other hand, the offspring from epiPGC-derived sperm showed normal imprinting profiles of both genes (Figure 6M). These findings demonstrate that epiPGCs specifically acquire the ability to erase the imprints, although not completely during the 132 hr culture, and suggest that when transplanted, they undergo complete erasure and re-establishment of the imprints as do PGCs in vivo (Chuma et al., 2005).

DISCUSSION

We have presented an integrated scenario that describes the roles of signaling molecules that confer the germ cell fate to epiblast cells. Unequivocally, germ cell specification is one of the events finely integrated in early embryonic patterning, in which a tight regulation of the actions of relevant signaling molecules plays decisive roles (Figure 7). Consistent with the previous findings showing the importance of the dosage of both Bmp4 and Blimp1 for PGC specification (Lawson et al., 1999; Ohinata et al., 2005; Vincent et al., 2005), BMP4 was here found to induce both *Blimp1* and *Prdm14* in the epiblast in a dose-dependent manner (Figures 2 and S10). Accordingly, in intact embryos, it is only from the area of the epiblast receiving the highest dosage of Bmp4 that the *Blimp1*-positive PGC precursors arise—that is, the most proximal posterior epiblast.

We demonstrated that Bmp2, which is structurally highly similar to Bmp4, induces *Blimp1* and *Prdm14* in the epiblast, although less efficiently than Bmp4 (Figure 2). The Bmp2 that has been shown to be expressed in the VE from ~E5.5 onward (Ying and Zhao, 2001) would therefore play the role of providing additional Bmp signaling to the proximal posterior epiblast to ensure/safeguard sufficient Bmp signaling levels for germ cell specification. Importantly, we provided multiple lines of evidence (Figures 1, 2, and 4) that Bmp8b controls (A)VE development, thereby restricting the AVE-derived inhibitory signals against germ cell specification to an appropriate level. A previous report showed that some unidentified factor(s) from the ExE suppress(es) the ectopic development of *Hex*-positive AVE within the VE (Rodriguez et al., 2005): Bmp8b could be one of these factors.

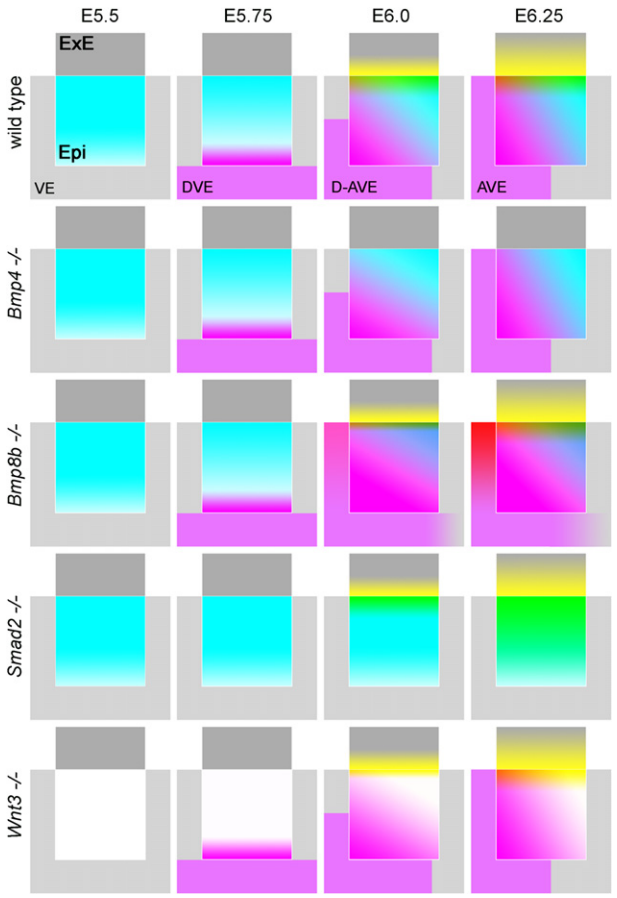

Figure 7. A Signaling Principle for the Germ Cell Fate

Grey, ExE; pale gray, VE; purple, distal (D) or anterior (A) VE; sky blue, epiblast with the ability to respond to Bmp4; white, epiblast lacking the ability to respond to Bmp4. Yellow, Bmp4 signal; red, inhibitory signals from DVE or AVE against posteriorization (including Cer1, Dkk1, Lefty1). The germ cell fate (green) is induced in the region where competent epiblasts receive sufficient Bmp4 signals.

Combined evidence (Figures 1 and 2) suggests that Bmp4 (and to a lesser extent, Bmp2) signals through the complex of Alk3 (or Alk6) and one of the type II receptors (most likely BmprII) via Smad1 and Smad5 in the epiblast for *Blimp1* and *Prdm14* expression, and hence for the germ cell fate. It is at present unknown whether the Smads activate *Blimp1* and *Prdm14* transcription directly or indirectly. Our preliminary evidence shows that the *cis*-regulatory region of *Blimp1* (~230 kb) contains multiple tissue-specific enhancers. Determination of the element(s) responsible for the *Blimp1* expression in the epiblast in response to BMP4 and examination of whether or not the Smads directly bind to and control *Blimp1* through the element(s) will be crucial

(J) Neonatal mice from 2-cell embryos in (I). Bright-field (left) and EGFP fluorescence (right) are shown.

(K–M) Imprinting methylation profiles of the *H19* and *Igf2r* loci in gonadal somatic cells, and male and female PGCs at E13.5 (K), in BV-negative and BV-positive cells (epiPGCs) induced for 132 hr (L), and in the tail fibroblasts of male and female offspring from epiPGC-derived sperm (M). Filled and open circles represent methylated and unmethylated CpGs, respectively, of the differentially methylated regions of the *H19* and *Igf2r* loci.

to provide a definitive answer to this question. Such experiments would also highlight whether the functions of Smad1 and Smad5 in PGC specification are redundant or distinctive.

In contrast to a previous report arguing that the Bmp4 signaling through the VE is obligatory for PGC specification (de Sousa Lopes et al., 2004), our present study demonstrated that Bmp4 signals directly onto the epiblast and the VE are dispensable for PGC specification (Figures 2 and 5). The discrepancy between the two studies might be related to the facts that 1) the previous study involved cultures with serum and feeder cells, which may complicate the interpretation of the data, and 2) the previous study relied primarily on AP staining for the detection of PGCs, which is a less strict criteria for PGCs. Nonetheless, the previous study showed that *Alk2* is essential for PGC specification. Phylogenetically, Bmp4 and Bmp2 belong to the DPP class of the Bmps, whereas Bmp8b belongs to the 60A class (Hogan, 1996). Generally, the former uses Alk3 or 6 as a type I receptor, while the latter uses Alk2. In this regard, Bmp8b may act through Alk2 in the VE to inhibit the proximal VE from differentiating into the DVE, which migrates anteriorly to form the AVE, a possibility that requires experimental verification.

Our experiments, on the other hand, demonstrated that the epiblasts bear the competence to form PGC-like cells in response to BMP4 only from E5.5 to E6.25 (Figures 3 and 5F). Coincidentally, Wnt3, which begins to be expressed in the epiblast at around E5.5 (Kemp et al., 2005), was shown to be a key factor conferring to the epiblasts the Bmp4 responsiveness (Figure 4). How Wnt3 might exert this function remains to be clarified. Notably, the expression levels of Bmp signal transducers in the *Wnt3*$^{-/-}$ epiblasts were comparable to those in the wild-type epiblasts (Figure S22). Further investigations are thus required to determine the molecular nature of the competence and the mechanism of actions of Wnt3 in its acquisition.

Essentially, BMP4 alone was sufficient to drive the epiblasts into epiPGCs. We noticed that after 36 hr culture, most epiblast cells showed BV, but some, especially those localizing at the outer surface, did not. The inability of a minority of cells to express BV in response to BMP4 may be due to their original heterogeneity (e.g., receptor expression, Smad expression, etc.) or some factor stemming from their topographic location in culture. The growth of the epiPGCs under a simple condition (LIF, SCF, and BMP4 in the SFM) was poor, with only ~400 such cells obtained after 132 hr (Figure 5). Given that 80% of the initial epiblast cells (~200 cells) began to express BV, the initial BV-positive cells divided only once during the 132 hr culture in this condition. Further addition of BMP8b and EGF enhanced the apparent growth of the epiPGCs, with ~1,250 such cells obtained after 132 hr (Figure 5). This is still smaller than the numbers of PGCs at a corresponding stage (~5,000–10,000 at E11.5), indicating that some critical requirements for the PGC growth are missing under our condition. The identification of such requirements is crucial for the more efficient propagation of PGCs or epiPGCs in vitro.

Remarkably, epiPGCs acquired the ability to erase the imprints, although not completely during the 132 hr culture. The timing of the erasure of imprints in PGCs coincides with their entry into the gonads, suggesting that some signals from gonadal somatic cells may trigger the erasure of imprints (Hajkova et al., 2002). However, our finding raises the important possibility that PGCs may undergo the erasure of imprints cell-autonomously without any cues from the genital ridges. Our culture system provides a powerful strategy by which to explore the mechanism of the erasure of the imprints. Finally, to our knowledge, our report is the first to demonstrate the generation of healthy offspring from gametes derived from pluripotent cells in culture and could serve as a basis for reconstructing the germ cell lineage with proper function in vitro.

EXPERIMENTAL PROCEDURES

The experimental procedures for establishing transgenic and knockout mouse strains, in situ hybridization, whole-mount immunofluorescence, immunohistochemical and AP staining, RNA isolation and RT-PCR, bisulfite sequencing, transplantation into seminiferous tubules, and ICSI are available in the Supplemental data.

Isolation and Serum-free Culture of Mouse Embryos

All the animals were treated with appropriate care according to the RIKEN ethics guidelines. Noon of the day when the vaginal plugs of mated females were identified was scored as E0.5. Female BDF1 mice were mated with male transgenic mice and were sacrificed at the designated stages (Downs and Davies, 1993) to recover embryos. Embryos were isolated in the dissection buffer (DMEM [Invitrogen] with 10% fetal bovine serum [FBS] [Stem Cell Science], 0.1 mM nonessential amino acids [NEAA], 1 mM sodium pyruvate, 100 U/ml penicillin, 0.1 mg/ml streptomycin, 2 mM L-glutamine, and 10 mM HEPES). For isolating the epiblasts, embryos were incubated with 0.5% trypsin and 2.5% pancreatin in Eagle's balanced salt solution (EBSS) (Invitrogen) for 7 min on ice. For inactivating the enzymes, embryos were then incubated in the dissection buffer for 2 min on ice. VE were removed by gentle pipetting with a mouth pipette (120 μm in diameter), and the ExE was cut off by a glass needle.

Isolated epiblasts were cultured in serum-free medium (SFM) (GMEM [Invitrogen] with 15% Knockout Serum Replacement [KSR] [Invitrogen], 0.1 mM NEAA, 1 mM sodium pyruvate, 0.1 mM 2-mercaptoethanol, 100 U/ml penicillin, 0.1 mg/ml streptomycin, 2 mM L-glutamine) in low-cell-binding U-bottom 96-well dishes (NUNC) at 37°C with 5% CO_2 for 36 hr to as long as 276 hr without or with cytokines. Medium was changed at 84 hr, 132 hr, 180 hr, and 228 hr of culture. The cytokines and chemical inhibitors used were purchased from Invitrogen, R&D, or Sigma.

Reconstruction of Embryonic Gonads and Transplantation into Germ Cell-Depleted Testes of Nude Mice

E13.5 male genital ridges (CD1) were isolated in the dissection medium, dissociated into single cells by TripLE (Invitrogen) treatment for 15 min at 37°C, plated onto a culture dish in the SFM, and incubated for 6 hr. The cells attached to the dishes were considered as gonadal somatic cells and were dissociated from the dish by TripLE (Invitrogen). At a corresponding time point, the cultured epiblasts with *acro/act*-EGFP bearing epiPGCs (BDF1xC57BL/6) were dissociated into single cells by TripLE (Invitrogen) and aggregated with the gonadal somatic cells prepared as above in low-cell-binding U-bottom 96-well dishes (NUNC) in the SFM for 2 days. We used 10 times as many gonadal somatic cells as epiPGCs for generating reconstructed gonads. The nude mice (ICR; Charles River) were treated with busulfan (40 mg/kg) at 4 weeks of age and were used as recipients after 1 week ~1 month following busulfan treatment. To avoid bone marrow failure, all recipient mice received bone marrow transplantation from untreated healthy donors within a week after busulfan treatment. The reconstructed gonads were transplanted under the tunica albuginea of the germ cell-depleted adult testes of the nude mice prepared as above.

SUPPLEMENTAL DATA

Supplemental Data include Supplemental Experimental Procedures, Supplemental References, seven tables, and twenty-two figures and can be found

with this article online at http://www.cell.com/supplemental/S0092-8674(09)00274-8.

ACKNOWLEDGMENTS

We thank B. Hogan and K. Lawson, K. Hayashi, R. Behringer, M. Nomura and En Li, and M. Yamamoto and H. Hamada, for the mutant mice for *Bmp4*, *Smad1*, *Wnt3*, *Smad2*, and *FoxH1*, respectively, and M. Okabe for the *acro/act*-EGFP transgenic strain. We also thank S. Aizawa and P. Q. Thomas for *Cer1* and *Hex* probes, respectively. We are grateful to the Animal Resources and Genetic Engineering Units for their support in deriving and maintaining the mice, and to the Genome Resource and Analysis Unit for their support in DNA sequencing. We thank D. Sipp for his help in manuscript preparation. Y.O. is a fellow in the Special Postdoctoral Researchers Program of RIKEN. This study was supported in part by a Grant-in-Aid from the MEXT of Japan, and by a PRESTO project grant from the JST.

Received: August 2, 2008
Revised: January 9, 2009
Accepted: March 5, 2009
Published: April 30, 2009

REFERENCES

Arnold, S.J., Maretto, S., Islam, A., Bikoff, E.K., and Robertson, E.J. (2006). Dose-dependent Smad1, Smad5 and Smad8 signaling in the early mouse embryo. Dev. Biol. *296*, 104–118.

Brennan, J., Lu, C.C., Norris, D.P., Rodriguez, T.A., Beddington, R.S., and Robertson, E.J. (2001). Nodal signalling in the epiblast patterns the early mouse embryo. Nature *411*, 965–969.

Chuma, S., Kanatsu-Shinohara, M., Inoue, K., Ogonuki, N., Miki, H., Toyokuni, S., Hosokawa, M., Nakatsuji, N., Ogura, A., and Shinohara, T. (2005). Spermatogenesis from epiblast and primordial germ cells following transplantation into postnatal mouse testis. Development *132*, 117–122.

de Sousa Lopes, S.M., Roelen, B.A., Monteiro, R.M., Emmens, R., Lin, H.Y., Li, E., Lawson, K.A., and Mummery, C.L. (2004). BMP signaling mediated by ALK2 in the visceral endoderm is necessary for the generation of primordial germ cells in the mouse embryo. Genes Dev. *18*, 1838–1849.

Dolci, S., Williams, D.E., Ernst, M.K., Resnick, J.L., Brannan, C.I., Lock, L.F., Lyman, S.D., Boswell, H.S., and Donovan, P.J. (1991). Requirement for mast cell growth factor for primordial germ cell survival in culture. Nature *352*, 809–811.

Downs, K.M., and Davies, T. (1993). Staging of gastrulating mouse embryos by morphological landmarks in the dissecting microscope. Development *118*, 1255–1266.

Farini, D., Scaldaferri, M.L., Iona, S., La Sala, G., and De Felici, M. (2005). Growth factors sustain primordial germ cell survival, proliferation and entering into meiosis in the absence of somatic cells. Dev. Biol. *285*, 49–56.

Ginsburg, M., Snow, M.H., and McLaren, A. (1990). Primordial germ cells in the mouse embryo during gastrulation. Development *110*, 521–528.

Hajkova, P., Erhardt, S., Lane, N., Haaf, T., El-Maarri, O., Reik, W., Walter, J., and Surani, M.A. (2002). Epigenetic reprogramming in mouse primordial germ cells. Mech. Dev. *117*, 15–23.

Hogan, B.L. (1996). Bone morphogenetic proteins: multifunctional regulators of vertebrate development. Genes Dev. *10*, 1580–1594.

Kemp, C., Willems, E., Abdo, S., Lambiv, L., and Leyns, L. (2005). Expression of all Wnt genes and their secreted antagonists during mouse blastocyst and postimplantation development. Dev. Dyn. *233*, 1064–1075.

Kurimoto, K., Yabuta, Y., Ohinata, Y., Shigeta, M., Yamanaka, K., and Saitou, M. (2008). Complex genome-wide transcription dynamics orchestrated by Blimp1 for the specification of the germ cell lineage in mice. Genes Dev. *22*, 1617–1635.

Lawson, K.A., Dunn, N.R., Roelen, B.A., Zeinstra, L.M., Davis, A.M., Wright, C.V., Korving, J.P., and Hogan, B.L. (1999). Bmp4 is required for the generation of primordial germ cells in the mouse embryo. Genes Dev. *13*, 424–436.

Lawson, K.A., and Hage, W.J. (1994). Clonal analysis of the origin of primordial germ cells in the mouse. Ciba Found. Symp. *182*, 68–84.

Lewis, S.L., Khoo, P.L., De Young, R.A., Steiner, K., Wilcock, C., Mukhopadhyay, M., Westphal, H., Jamieson, R.V., Robb, L., and Tam, P.P. (2008). Dkk1 and Wnt3 interact to control head morphogenesis in the mouse. Development *135*, 1791–1801.

Liu, P., Wakamiya, M., Shea, M.J., Albrecht, U., Behringer, R.R., and Bradley, A. (1999). Requirement for Wnt3 in vertebrate axis formation. Nat. Genet. *22*, 361–365.

Matsui, Y., Toksoz, D., Nishikawa, S., Williams, D., Zsebo, K., and Hogan, B.L. (1991). Effect of Steel factor and leukaemia inhibitory factor on murine primordial germ cells in culture. Nature *353*, 750–752.

Nagy, A., Gertsenstein, M., Vintersten, K., and Behringer, R. (2003). Manipulating the Mouse Embryo, Third Edition edn (New York: Cold Spring Harbor Laboratory Press).

Nomura, M., and Li, E. (1998). Smad2 role in mesoderm formation, left-right patterning and craniofacial development. Nature *393*, 786–790.

Ohinata, Y., Payer, B., O'Carroll, D., Ancelin, K., Ono, Y., Sano, M., Barton, S.C., Obukhanych, T., Nussenzweig, M., Tarakhovsky, A., et al. (2005). Blimp1 is a critical determinant of the germ cell lineage in mice. Nature *436*, 207–213.

Ohinata, Y., Sano, M., Shigeta, M., Yamanaka, K., and Saitou, M. (2008). A comprehensive, non-invasive visualization of primordial germ cell development in mice by the Blimp1-mVenus and stella-ECFP double transgenic reporter. Reproduction *136*, 503–514.

Ohta, H., Yomogida, K., Yamada, S., Okabe, M., and Nishimune, Y. (2000). Real-time observation of transplanted 'green germ cells': proliferation and differentiation of stem cells. Dev. Growth Differ. *42*, 105–112.

Perea-Gomez, A., Vella, F.D., Shawlot, W., Oulad-Abdelghani, M., Chazaud, C., Meno, C., Pfister, V., Chen, L., Robertson, E., Hamada, H., et al. (2002). Nodal antagonists in the anterior visceral endoderm prevent the formation of multiple primitive streaks. Dev. Cell *3*, 745–756.

Rodriguez, T.A., Srinivas, S., Clements, M.P., Smith, J.C., and Beddington, R.S. (2005). Induction and migration of the anterior visceral endoderm is regulated by the extra-embryonic ectoderm. Development *132*, 2513–2520.

Saitou, M. (2009). Specification of the germ cell lineage in mice. Front. Biosci. *14*, 1068–1087.

Saitou, M., Barton, S.C., and Surani, M.A. (2002). A molecular programme for the specification of germ cell fate in mice. Nature *418*, 293–300.

Sato, M., Kimura, T., Kurokawa, K., Fujita, Y., Abe, K., Masuhara, M., Yasunaga, T., Ryo, A., Yamamoto, M., and Nakano, T. (2002). Identification of PGC7, a new gene expressed specifically in preimplantation embryos and germ cells. Mech. Dev. *113*, 91–94.

Seki, Y., Yamaji, M., Yabuta, Y., Sano, M., Shigeta, M., Matsui, Y., Saga, Y., Tachibana, M., Shinkai, Y., and Saitou, M. (2007). Cellular dynamics associated with the genome-wide epigenetic reprogramming in migrating primordial germ cells in mice. Development *134*, 2627–2638.

Shi, Y., and Massague, J. (2003). Mechanisms of TGF-beta signaling from cell membrane to the nucleus. Cell *113*, 685–700.

Tam, P.P., and Loebel, D.A. (2007). Gene function in mouse embryogenesis: get set for gastrulation. Nat. Rev. Genet. *8*, 368–381.

Tam, P.P., and Snow, M.H. (1981). Proliferation and migration of primordial germ cells during compensatory growth in mouse embryos. J. Embryol. Exp. Morphol. *64*, 133–147.

Thomas, P.Q., Brown, A., and Beddington, R.S. (1998). Hex: a homeobox gene revealing peri-implantation asymmetry in the mouse embryo and an early transient marker of endothelial cell precursors. Development *125*, 85–94.

Tsutsui, H., Karasawa, S., Shimizu, H., Nukina, N., and Miyawaki, A. (2005). Semi-rational engineering of a coral fluorescent protein into an efficient highlighter. EMBO Rep. *6*, 233–238.

Vincent, S.D., Dunn, N.R., Sciammas, R., Shapiro-Shalef, M., Davis, M.M., Calame, K., Bikoff, E.K., and Robertson, E.J. (2005). The zinc finger transcriptional repressor Blimp1/Prdm1 is dispensable for early axis formation but is required for specification of primordial germ cells in the mouse. Development *132*, 1315–1325.

Yabuta, Y., Kurimoto, K., Ohinata, Y., Seki, Y., and Saitou, M. (2006). Gene expression dynamics during germline specification in mice identified by quantitative single-cell gene expression profiling. Biol. Reprod. *75*, 705–716.

Yamaji, M., Seki, Y., Kurimoto, K., Yabuta, Y., Yuasa, M., Shigeta, M., Yamanaka, K., Ohinata, Y., and Saitou, M. (2008). Critical function of Prdm14 for the establishment of the germ cell lineage in mice. Nat. Genet. *112*, 11306–11311.

Yamamoto, M., Meno, C., Sakai, Y., Shiratori, H., Mochida, K., Ikawa, Y., Saijoh, Y., and Hamada, H. (2001). The transcription factor FoxH1 (FAST) mediates Nodal signaling during anterior-posterior patterning and node formation in the mouse. Genes Dev. *15*, 1242–1256.

Ying, Y., Liu, X.M., Marble, A., Lawson, K.A., and Zhao, G.Q. (2000). Requirement of Bmp8b for the generation of primordial germ cells in the mouse. Mol. Endocrinol. *14*, 1053–1063.

Ying, Y., and Zhao, G.Q. (2001). Cooperation of endoderm-derived BMP2 and extraembryonic ectoderm-derived BMP4 in primordial germ cell generation in the mouse. Dev. Biol. *232*, 484–492.